Pathology - Research and Practice 246 (2023) 154499

Contents lists available at ScienceDirect

Pathology - Research and Practice

journal homepage: www.elsevier.com/locate/prp

Ellagic acid increases implantation rates with its antifibrotic effect in the rat model of intrauterine adhesion

Gulistan Sanem Saribas [a,b,*,1], Ozen Akarca Dizakar [c], Candan Ozogul [d], Ekin Celik [e], Mahmut Cerkez Ergoren [f]

[a] University of Health Sciences, Gulhane Faculty of Medicine, Department of Histology and Embryology, Ankara, Turkey
[b] Kirsehir Ahi Evran University, Faculty of Medicine, Department of Histology and Embryology, Kirsehir, Turkey
[c] Izmir Bakircay University, Faculty of Medicine, Department of Histology and Embryology, Izmir, Turkey
[d] University of Kyrenia, Faculty of Medicine, Department of Histology and Embryology, Kyrenia, Northern Cyprus, Turkey
[e] Kirsehir Ahi Evran University, Faculty of Medicine, Department of Medical Biology, Kirsehir, Turkey
[f] Near East University, Faculty of Medicine, Department of Medical Biology, Nicosia, Northern cyprus, Turkey

ARTICLE INFO

Keywords:
Asherman Syndrome
Ellagic acid
Fibrosis
Intrauterine adhesion

ABSTRACT

Intrauterine adhesions (IUA) are defined as the adhesion of opposing endometrial tissue with dense fibrous adhesive bands within the uterine cavity. With the increase in cesarean sections and endometrial surgical procedures, intrauterine adhesions have become a problem with increasing incidence and decreasing implantation. The purpose of the study was to investigate the effect of ellagic acid (EA), a phenolic compound, on fibrosis in IUA model rats. Another goal of the study was to increase endometrial receptivity with EA. The groups in the study were planned as control, DMSO, EA, IUA, IUA+DMSO, and IUA+EA, with 8 Sprague Dawley rats in each group. EA was administered at a dose of 100 mg/kg/day for 35 days. At the end of the experiment, the uterine tissues of the rats were removed. Histochemical staining was used to validate the IUA model and determine the degree of fibrosis. The levels of some fibrosis-related genes and proteins in the obtained uterine tissues were evaluated. In addition, implantation rates were determined. In our findings, it was observed that the fibrotic structure was decreased in the treated IUA+EA group compared to the IUA group, while fibrotic improvement was supported by down-regulation of TGFβ1 activity and up-regulation of BMP7 activity. The increase in the expression of the endometrial marker LIF with EA treatment was consistent with the increase in implantation rates with treatment. As a result of the study, it can be said that EA applied as a treatment against IUA causes healing in uterine tissue by reducing fibrosis and increases implantation rates by increasing endometrial receptivity.

1. Introduction

Intrauterine adhesions (IUA) are described as the adhesion of opposing endometrial tissue with dense fibrous sticky bands inside the uterine cavity [1,2]. Any event that will damage the endometrium's basal layer has the potential to create an intrauterine adhesion and Asherman's syndrome [3,4]. A few cases of Asherman's syndrome treatment with the hysterotomy approach have been reported in the past and that there was sufficient improvement in the endometrium for reproductive functions. However, the hysteroscopic approach is not preferred today due to its great risks. Instead of this, the use of hysteroscopy techniques is accepted today. Hysteroscopy not only confirms the diagnosis of intrauterine adhesions, but also provides treatment. Many complications can be observed during hysteroscopy. The main problem that can be encountered is the recurrence of adhesion formation. Even in severe adhesion cases, this rate goes up to 63% [5,6]. The loss of the stem cell population located in the basalis layer of the endometrium and deep traumas in the underlying myometrium layer are thought to be the cause of functional failure in the functional layer of the endometrium in Asherman syndrome [7]. Angiogenesis and revascularization abilities decrease in IUA patients, while the expression of adhesion-related cytokines increases [8]. Some changes are observed in

* Correspondence to: University of Health Sciences, Gul hane Faculty of Medicine Department of Histology and Embryology, Dean's building room no:6, Ankara, Turkey.
E-mail address: sanemarik@gmail.com (G.S. Saribas).
[1] ORCID: 0000–0001-7582–6235

https://doi.org/10.1016/j.prp.2023.154499
Received 7 April 2023; Received in revised form 25 April 2023; Accepted 2 May 2023
Available online 3 May 2023

the endometrium, which shows adhesion formation histologically. The most important change leading to dysfunction is the replacement of endometrial stroma with fibrous tissue [9,10]. The fibrotic-antifibrotic mechanism in tissues is very diverse. According to current research, BMP7 is a protective mechanism against TGFβ-mediated profibrogenic signaling [11–13].

Ellagic acid (EA) is a polyphenolic compound found in a variety of fruits and vegetables. It has been shown in-vivo and in-vitro studies to have anti-aging, anti-proliferative, anti-fibrotic, anti-atherosclerotic, anti-cancer, and anti-mutagenic properties in addition to a strong anti-oxidant property with free radical scavenging ability [14–16].

Intrauterine adhesions have become an increasingly serious problem with the increasing number of cesarean sections and operative endometrial procedures and the expansion of diagnostic possibilities. Today, new methods and agents are being developed to reduce or prevent intrauterine adhesion. For this reason, we investigated the possible curative effects of ellagic acid in rats, for which an IUA model was created in our study, in order to investigate new treatment possibilities. It is thought that EA application may lead to improved reproductive results with the decrease of fibrotic structure observed in IUA and changes in the expression of leukemia inhibitory factor (LIF), an endometrial receptivity marker.

2. Material and methods

A total of 80 female Sprague-Dawley rats in the co-cycle (oestrus), 8–10 weeks old, non-pregnant, and weighing 200–250 g, were used in the study. First of all, the intrauterine adhesion model was proven by fibrosis/adhesion control in 2 rats. Forty-eight animals were included in the experimental groups. A total of 48 rats, 8 in each group, were used for the analysis of the tissues obtained. Thirty female rats were used for the reproductive function test. Approval for this study was obtained from the Kobay DHL A.Ş. Local Ethics Committee (Approval date and no: 04.04.2019, 372).

2.1. Creating an intrauterine adhesion model with uterine trauma

First, two rats were used to establish and validate the IUA rat model. After the rats were injected with ketamine (45 mg/kg) and xylazine (5 mg/kg) intramuscularly and anesthetized, the abdominal walls of the rats were opened with a vertical incision and the uterine horns were visualized. An incision was made at the utero-tubal junction to traumatize the uterine horns. The 16-gauge standard needle tip was inserted through the utero-tubal junction and advanced up to 2/3 of the uterus lumen, and 4 rotations and withdrawals were applied 4 times in succession [17]. After the trauma, the uterus was placed in the abdomen and the abdomen was closed. After 2 weeks (3 oestrus cycles) after the IUA model application, the subjects were sacrificed and their uterine tissues were removed, and the model was proven by performing hematoxylin-eosin (H&E) staining after routine histological follow-ups (model formation corresponds to 2 weeks after the traumatization process) (Figs. 1 and 2).

2.2. Administration of ellagic acid

For 35 days, elagic acid (sc-202598A, Santa Cruz Biotech) (100 mg/kg/day) dissolved in 0.2% dimethyl sulfoxide (DMSO) was administered orally via an intragastric tube in a volume of 2 mL [18–20].

2.3. Experimental groups

The rats were maintained in separate cages at a standard temperature (22–24 ºC) with a 12-hour light/dark cycle and standard rat chow. Rats were divided into 6 groups:

Control group (n = 8): Stress was created by applying the an incision procedure to healthy rats. Gavage stress was applied with 2 mL of SF for 35 days.

Fig. 1. IUA induction in rats.

DMSO group (n = 8): Stress was created by incision procedure in healthy rats and 2 mL of EA solvent (0.2% DMSO) was given orally for 35 days.

EA group (n = 8): Stress was created by incision in healthy rats and 2 mL of dissolved EA (100 mg/kg/day) was given orally for 35 days.

IUA group (n = 8): After the IUA model was formed, gavage stress was applied with 2 mL of SF for 35 days.

IUA+DMSO group (n = 8): After the IUA model was formed, 2 mL of 0.2% DMSO was administered orally for 35 days.

IUA+EA group (n = 8): After the IUA model was formed, 2 mL of dissolved EA (100 mg/kg/day) was administered orally for 35 days.

The rats of all groups were sacrificed at the end of the 35th day and their uterine tissues were taken. The right horn of the uterine tissues was used for RNA isolation, and the left horn was used for histochemical and immunohistochemical analysis.

2.4. Histochemical method

Uterine tissue samples were fixed in 10% neutral formalin solution for light microscopic examination. After routine follow-up procedures, Masson's trichrome staining was applied to the sections of 4–5 μm thickness obtained from the paraffin blocks prepared for each animal in all groups. For each sample, the percentage of blue area pixels was calculated with Image J program and the percentage of fibrotic area was determined [17].

2.5. RNA isolation and qRT-PCR

Prior to the isolation step, tissues were homogenized using homogenizator (Domel, Millmix 20). The total RNA were extracted using the Zymo Research Quick-RNA Mini Prep (USA) kit. After DNAseI treatment, concentrations of the obtained RNAs were determined using a UV-Vis

Fig. 2. Healthy uterine tissue of the control group (A); IUA model with stenosis and synechiae in the uterine lumen (B, C) (cross section; H&E; X40).

spectrophotometer (Nanodrop 2000/2000c, Thermo Fisher Sci.) device and diluted to 80 ng/µL for each sample. Complementary DNA was synthesized from the isolated RNAs using the Revert Aid First Strand cDNA Synthesis Kit (Thermo Scientific, USA) using PCR device (Veriti, Applied Biosystems). qPCR analysis was performed using SYBR Green Master Mix (Applied Biosystems, USA) in QuantStudio 5, Applied Biosystems instrument with QuantStudio Real Time PCR Software. GAPDH gene was used as a reference gene and comparative Ct method ($2^{-\Delta\Delta Ct}$) was used to analyse the results. The primer sequences used in the experiment are listed in Table 1.

2.6. Immunohistochemical assay

Sections of 4 µm thickness taken on polylysine slides were deparaffinized and dehydrated. Then the tissues were incubated with pH 6.0 citrate buffer and 3% hydrogen peroxide. After the blocking step with UltraV block (TP-125-HL, Thermo Sci.), the sections were incubated with at TGFβ1 (bs-0086R, rabbit polyclonal, Bioss Inc.), BMP7 (bs-2242R, rabbit polyclonal, Bioss Inc.), and LIF (bs-1058R, rabbit polyclonal, Bioss Inc.) primary antibodies at 1:200 dilution at 4ºC overnight. Then, according to the protocol, an anti-mouse and anti-rabbit IgG HRP secondary kit (TP-125-BN, Thermo Fisher Scientific) was used. Finally, the sections were incubated for 5–10 min with aminoethyl carbazole (AEC) substrate. After allowing the visible immune reaction to occur under the microscope, Mayer's hematoxylin was used as a background stain. Sections closed using a water-based closure medium were evaluated in a computer-assisted imaging system. At the end of the evaluations, immunohistochemical uptake densities for each primary antibody were determined as percentages in the Image J program and statistical data were generated [17].

2.7. Reproductive functionality test

Control (n = 10), IUA (n = 10) and IUA+EA (n = 10) groups were used for the reproductive functionality test. At the end of day 35, rats were caged overnight with male rats (ratio 3:1) and a vaginal smear was performed on each female rat the next morning to determine the presence of sperm. The presence of sperm was accepted as proof of mating and day 0.5 was determined as postcoitum day. Pregnant rats were excised at 13.5 postcoitum days. The number of implanted embryos in each uterine corn was determined.

Table 1
RT-PCR Primer Sequences (Genbank ID: NM_021578.2 for TGFB1; NM_001191856.2 for BMP7; XM_008770359.2 for LIF; XM_017593963.1 for GAPDH).

Gene	Forward	Reverse
TGFβ1	CTACTGCTTCAGCTCCACAG	GCACTTGCAGGAGCGCAC
BMP7	CGCCCATGTTCATGTTGGAC	TCGATGGTGGTATCGAGGGT
LIF	CGCCCAACATGACGGATTTC	TTGTTGCACAGACGGCAAAG
GAPDH	ACAGTCCATGCCATCACTGCC	GCCTGCTTCACCACCTTCTTG

2.8. Statistical analysis

Statistical analyses for histological, immunohistochemical, and reproductivity results were performed using IBM SPSS Statistics 21 (IBM Corp. Released 2012. IBM SPSS Statistics for Windows, Version 21.0. Armonk, NY). Data distribution was evaluated by the Shapiro-Wilk test. Independent data that did not show a normal distribution were evaluated with the Kruskal-Wallis test. When there was a statistically significant difference between the groups, the Bonferroni corrected Mann-Whitney U test was used to identify the different group. p values < 0.05 were considered statistically significant. Statistical analyses for gene expression results were performed using GraphPad Prism software version 6 (GraphPad Software, La Jolla, USA). Student T-test and ANOVA tests were performed for statistical analysis. p values of at least less than 0.05 were considered significant. Levels of significance were represented as follows: $p > 0.05$ as not significant, $p \leq 0.05$ as * , $p \leq 0.01$ as * *, $p \leq 0.001$ as * ** , and $p \leq 0.0001$ as * ** *.

3. Results

3.1. Histological results

The images obtained by Masson's trichrome staining at X40 magnification were used to calculate the fibrotic area of the uterine sections of all groups. The mean and standard deviation values of the fibrotic area in the uterus were found to be 24.3 ± 4.3 in the control group, 27.6 ± 3.3 in the DMSO group, 22.1 ± 4.7 in the EA group, 57.0 ± 7.7 in the IUA group, 55.4 ± 7.7 in the IUA+DMSO group, and 35.0 ± 7.6 in the IUA+EA group.

When the control group and other groups were compared, only the fibrosis areas in the IUA and IUA+DMSO groups showed a statistically significant increase compared to the control group (respectively, $p = 0.001$; 0.002). Similarly, the increase in the untreated groups (IUA and IUA+DMSO) was statistically significant compared to the DMSO group (respectively, $p = 0.024$; 0.038). Compared to the EA group, the increase in the IUA and IUA+DMSO groups also showed a statistically significant increase (respectively, $p < 0.001$; <0.001). When the IUA group and the IUA+DMSO group were compared with the treatment group (IUA+EA), although the difference between them was not statistically significant, the percentage of fibrotic area decreased in the treatment group ($p = 0.504$; 0.712, respectively) (Figs. 3 and 4).

3.2. Gene expression results

In RT-PCR experiments, no significant difference was found between the control group and DMSO group for TGFβ1, BMP7 and LIF genes ($p > 0.05$) (Fig. 5). Considering the genetic inactivity of DMSO, the results are consistent with the literature. Similarly, it was shown that EA

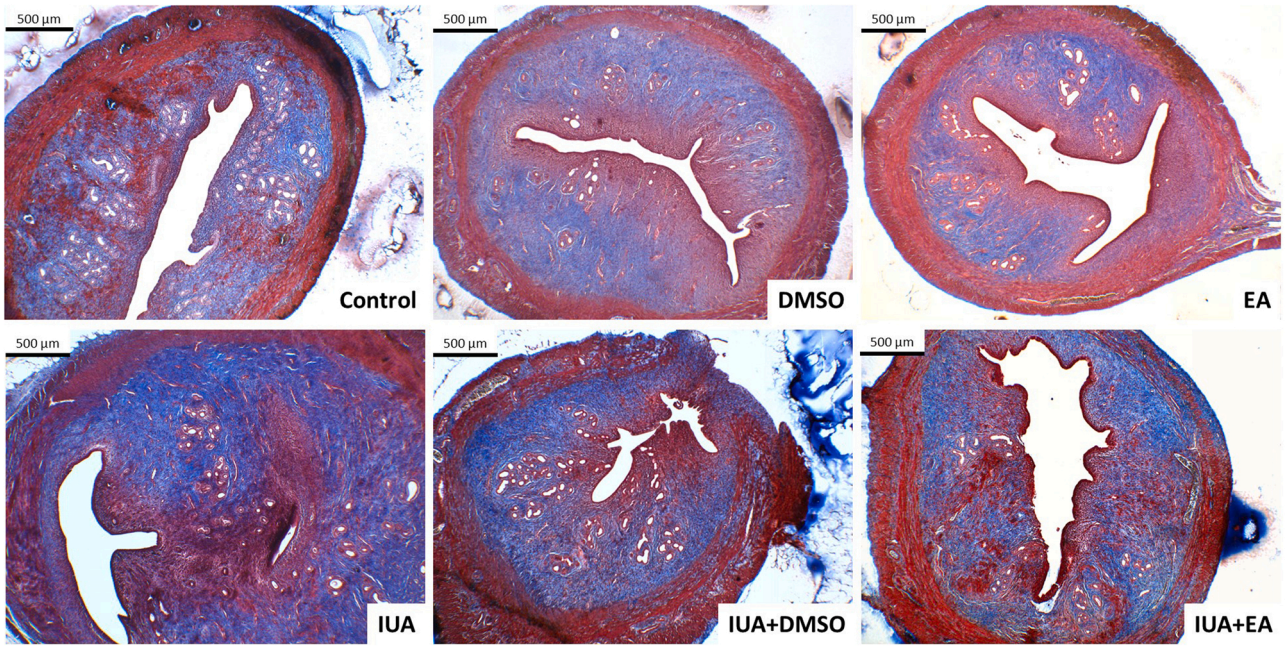

Fig. 3. Representative photographs of Masson's trichrome staining of all groups. The abundance of blue pixel areas in the IUA and IUA+DMSO groups indicates the intensity of fibrosis severity (X40).

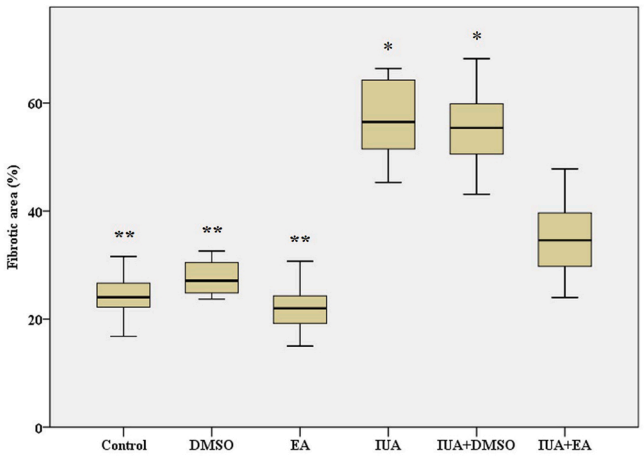

Fig. 4. Quantitative summary of fibrotic area by Masson's trichrome staining (*: significant with control group, **: significant with IUA group, $p < 0.05$).

applied to healthy animals did not cause a significant difference in gene expression compared to the control group. This shows that EA cannot be considered as a preventive treatment ($p > 0.05$).

TGFβ1, one of the most important fibrosis markers, showed a significant increase in the IUA group compared to the control group ($p < 0.0001$) (Fig. 5A). There was a significant decrease in BMP7 and LIF gene expressions in the IUA group compared to the control group ($p < 0.01$; $p < 0.001$, respectively) (Fig. 5B,C). This is proof that the disease model has been successfully established. In addition, the success of EA treatment after IUA injury was proven by a significant decrease in TGFβ1 gene expressions and significant increases in BMP7 and LIF gene expressions ($p < 0.0001$). No significant difference was observed in the gene expression levels of the IUA+DMSO group compared to the IUA group. This supports the therapeutic potential of EA.

3.3. Immunohistochemical results

The percentage of immunopositivity of BMP7, LIF and TGFβ1 antibodies of each rat was calculated with the Image J program. Images obtained from X400 magnification were used in the evaluation.

When TGFβ1 immunopositivity rates were evaluated in uterine

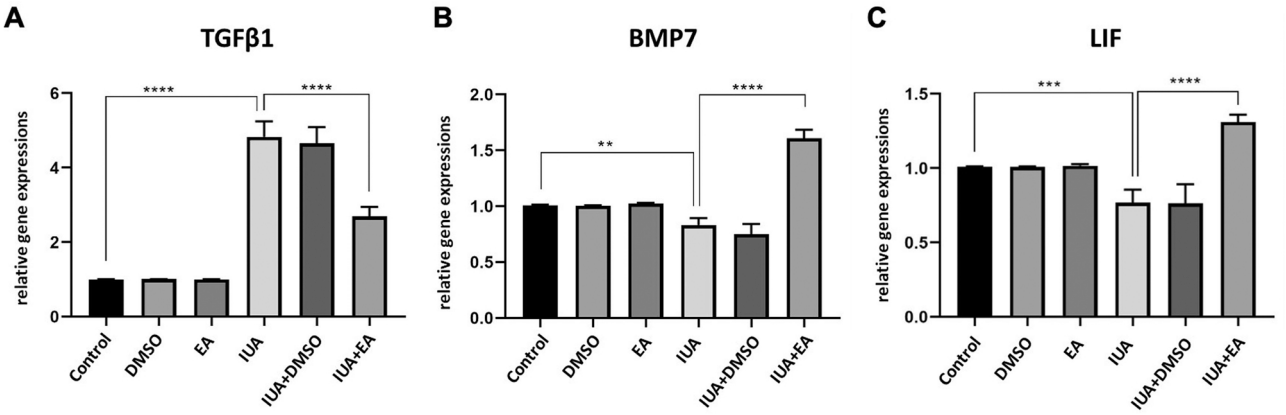

Fig. 5. Quantitative summary of relative gene expressions A. TGFβ1 B. BMP7 C. LIF (**$p < 0.01$; ***$p < 0.001$, and ****$p < 0.0001$).

tissue, there was no significant difference between the control group and the DMSO, EA, and IUA+EA groups ($p = 1.000$; 0.138; 0.433, respectively), while TGFβ1 protein expression levels increased significantly in the IUA and IUA+DMSO groups compared to the control group ($p < 0.001$). When the EA and DMSO groups were compared with the IUA model and the treated group, an increase in TGFβ1 expression was observed in the treatment group and this increase was statistically significant for the EA group ($p < 0.001$). It was observed that the TGFβ1 protein level of the treatment group was statistically significantly lower compared to the untreated IUA and IUA+DMSO groups ($p = 0.029$; 0.012, respectively) (Figs. 6 and 7). These results were supported by increased fibrosis in IUA modeled tissues with increased TGFβ1 levels, and it was determined that the fibrotic marker TGFβ1 activity decreased significantly in the EA-treated group but was not statistically different from the control group.

When BMP7 immunostaining was evaluated, there was no significant difference between the DMSO and EA groups when compared to the control group ($p = 1.000$; 1.000, respectively), while the BMP7 expression levels in the IUA model groups showed a statistically significant decrease ($p < 0.001$). Although there was a statistically significant decrease in BMP7 expression in the treatment group when the EA and DMSO groups were compared with the IUA+EA group, it was observed that the treatment group increased statistically significantly compared to the IUA and IUA+DMSO groups (Figs. 6 and 7). Based on these findings, it was determined that BMP7 activity was downregulated in the IUA group, which mediates a mechanism opposite to TGF-mediated profibrogenic signaling.

When the immunostaining rates of LIF, which is an endometrial receptivity marker, were evaluated, there was no significant difference between the control group and the DMSO group, and between the control group and the EA group ($p = 1.000$; 1.000, respectively), while LIF expression levels showed a statistically significant decrease in the IUA model groups (IUA, IUA+DMSO, and IUA+EA) ($p < 0.001$; <0.001; $p = 0.002$, respectively).

When the EA and DMSO groups were compared with the IUA model and the treated group, decreased LIF expression was observed in the treatment group, and this decrease was statistically significant for the EA group ($p < 0.001$). It was observed that the LIF protein level of the treatment group increased statistically significantly compared to the untreated IUA and IUA+DMSO groups ($p = 0.042$; 0.005, respectively) (Figs. 6 and 7). With these results, it was determined that endometrial receptivity decreased significantly in the IUA model group and LIF, an endometrial marker, increased statistically significantly with EA treatment.

3.4. Reproductivity results

Implanted embryos were counted to determine differences in reproductive functionality in the IUA groups after treatment with EA (Figs. 8 and 9). The mean number of implanted embryos was 15.00 ± 1.70 in the control group, 4.40 ± 1.43 in the IUA group, and 9.70 ± 2.36 in the IUA+EA group. When the embryo numbers were evaluated, it was seen that there was a statistical difference between all groups. Compared to the control group, the number of implanted embryos in the IUA and IUA+EA groups showed a statistically significant decrease ($p < 0.001$; $p = 0.043$, respectively). The number of implanted embryos in the treatment group showed a statistically significant increase compared to the IUA group.

4. Discussion

Intrauterine adhesions are defined as the adhesion of opposing

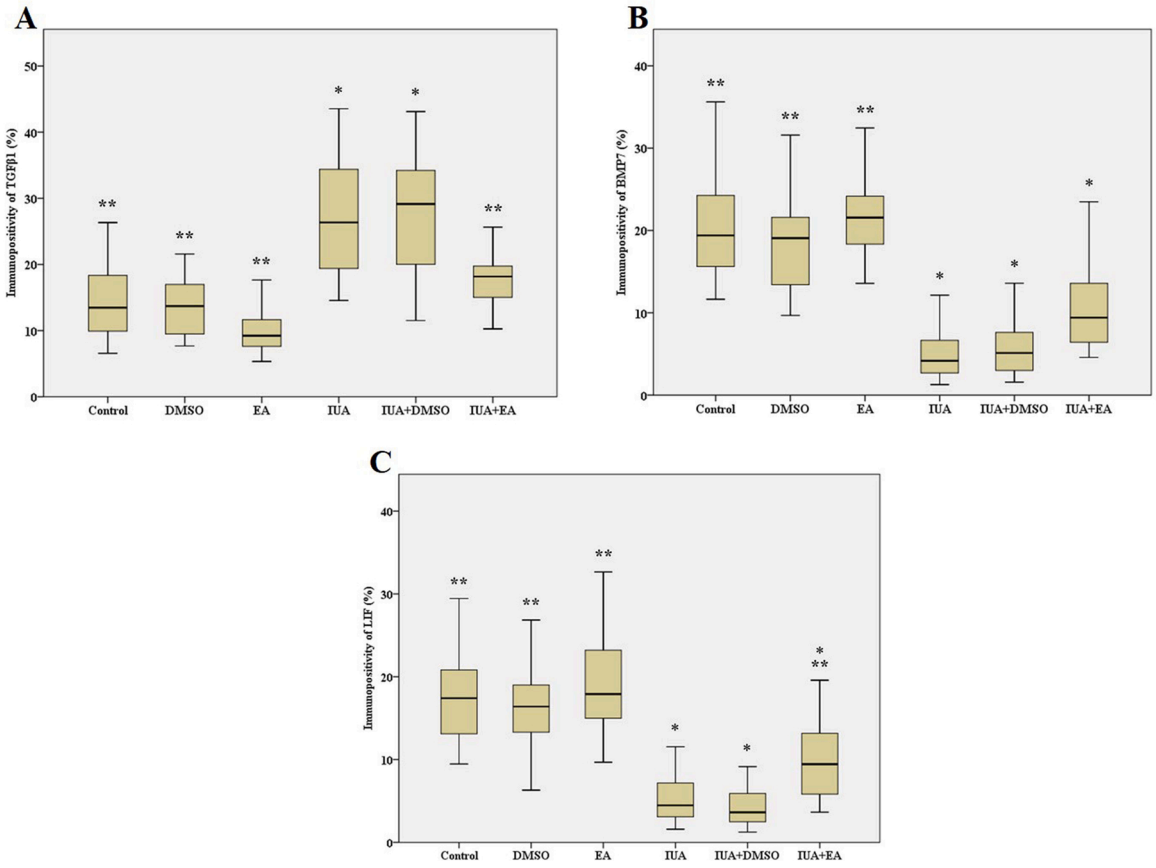

Fig. 6. TGFβ1 (A), BMP7 (B) and LIF (C) immunopositivity rates in uterine tissues of all groups (*: significant with control group, **: significant with IUA group, $p < 0.05$).

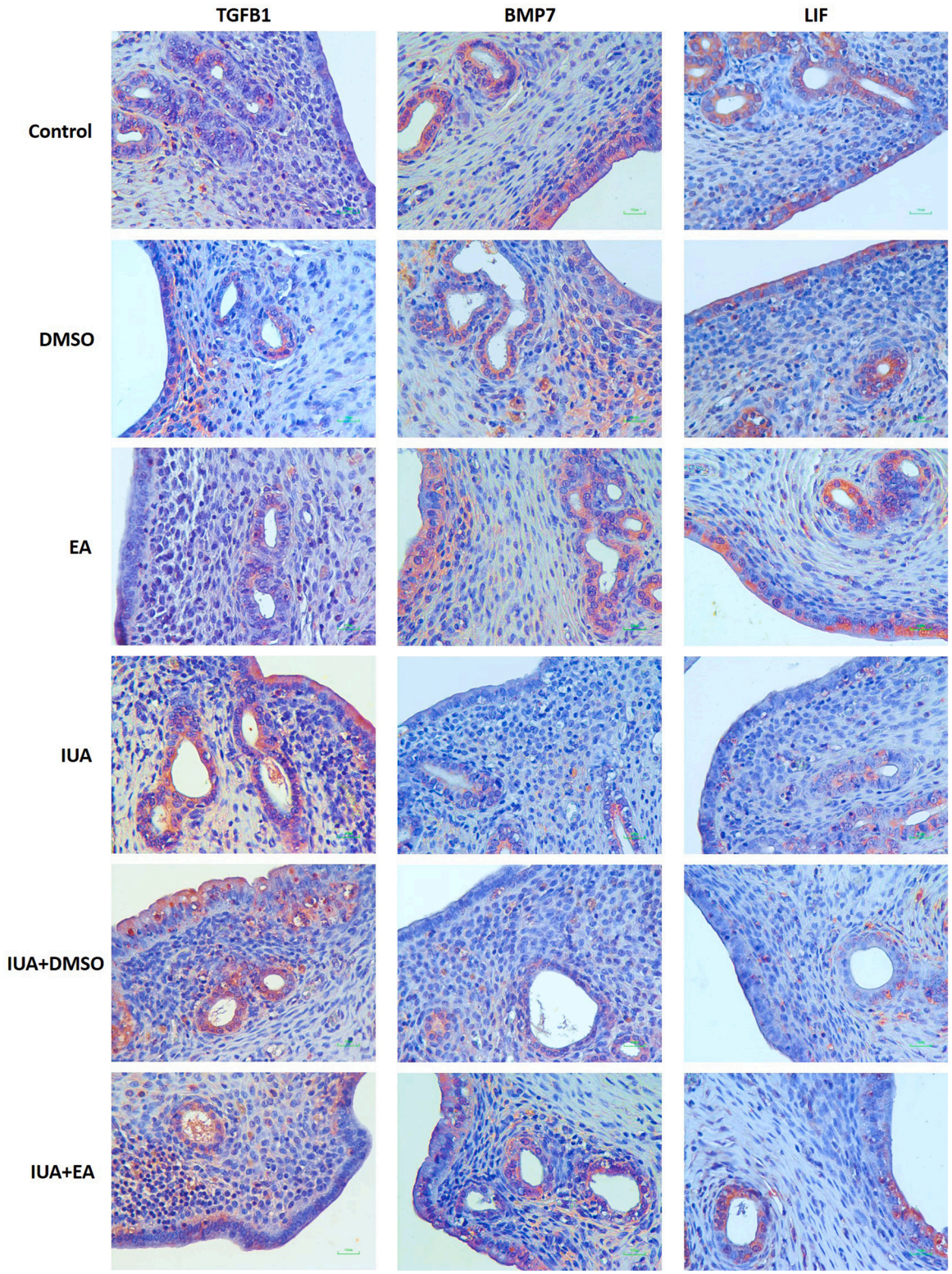

Fig. 7. Representative immunostaining images of various primary antibodies in uterine tissues of all groups (n = 8; each group) (AEC-hematoxylin; X400).

endometrial tissue with dense fibrous adhesive bands within the uterine cavity. Any event that will damage the endometrium's basal layer can form as an intrauterine adhesion and lead to Asherman's syndrome. IUA is mostly formed after surgical procedures such as dilatation and curettage or endometrial cavity-related myomectomy, septal resection, and cesarean section [21,22]. Angiogenesis and revascularization abilities decrease in IUA patients, while the expression of adhesion-related cytokines increases [23]. Some changes are observed in the endometrium, which shows adhesion formation histologically. The endometrial stroma is replaced by fibrous tissue, the epithelial glands are inactive in the form of cubo-columnar epithelium, and the distinction between the basal and functional layers disappears [9,10].

The true prevalence of IUA is difficult to ascertain. Because this is a rare and asymptomatic event in the general population [3,4]. In a study

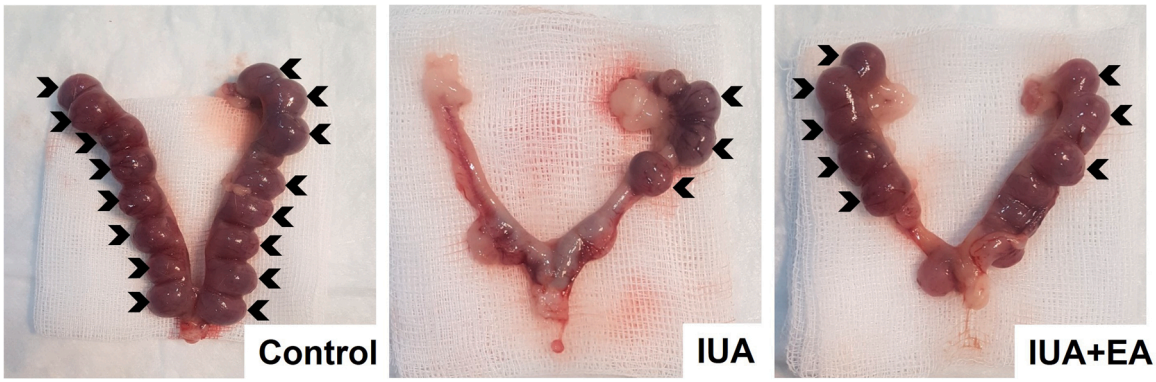

Fig. 8. Representative images showing pregnancy outcomes of rats in the control, model (IUA), and treatment (IUA+EA) groups; implanted embryo (arrowhead) (n = 10; in each group).

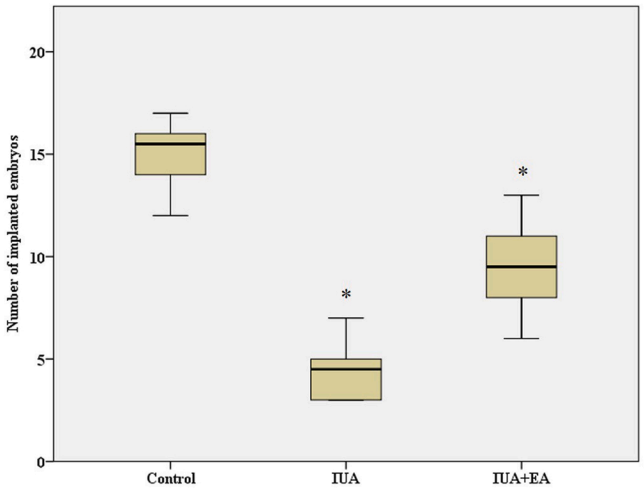

Fig. 9. Number of implanted embryos (*: significant with control group, $p < 0.05$).

in which a large number of IUA cases were investigated, it was determined that 67% of the cases were formed after abortion or curettage was applied as a result of early pregnancy loss. While the rate of IUA after cesarean delivery is around 2% [8], this rate rises to 39% in recurrent pregnancy losses [24]. Its incidence is around 40–60% in postpartum curettage cases. Furthermore, studies have shown that the number of curettages increases the frequency and severity of IUA [25]. According to a study, after in vitro fertilization, the prevalence of IUA rose by up to 38% in women who experienced early pregnancies losses [5].

According to a study by Gambadauro et al., intrauterine adhesions may form after conservative treatment for uterine fibroids. According to this article, intrauterine adhesions were thought to be a possible side effect of the conservative management of fibroids [26]. Hysteroscopic myomectomy may cause adhesions in the endometrium due to the trauma caused by surgery, and even in some cases, such as multiple fibroids, the severity of adhesions is higher [6]. Recurrent pregnancy loss is often caused by partial obstructions in the tuba uterina and uterine cavity, where fibrotic adhesions and poor vascularization are observed. Some researchers argue that there is a decrease in myometrial contractility and weakening of vascularity due to fibrosis, and therefore sex steroids cannot affect the endometrial tissue. As a result, adhesions cause atrophic endometrium [27,28].

It has been found in numerous studies that BMP7 is a mechanism against TGFβ-mediated pro-fibrogenic signaling and that BMP7 activity is down-regulated in fibrotic tissues, despite the fact that the fibrotic-antifibrotic mechanism in tissues is quite different. Liver fibrosis model studies have shown the efficacy of exogenous BMP7 treatment in reducing important parameters including TGFβ/Smad signaling and hepatic stellate cell activation [11,12]. In addition, a herbal substance has been proven to be successful at reducing hepatic fibrosis by enhancing phosphorylated Smads levels and BMP7 antifibrotic signaling in experiments to uncover regulators of BMP7/Smad signaling [29]. Several studies have shown that overexpression of BMP7 protects against fibrosis damage caused by TGF and Smad pathways in variety of organs, including the heart, lung, and kidney [30–32].

In our study, when we evaluated the fibrotic pathway in terms of TGFβ1 and BMP7 genes and proteins in the intrauterine adhesion model, we revealed significantly increased expression of TGFβ1 and significantly decreased expression of BMP7. These findings were also supported by the increased collagen density in Masson's trichrome staining results.

EA is a polyphenolic substance present in a wide variety of fruits and vegetables. The effects of EA on the regulation of multiple pathways can be summarized as follows: activation of the antioxidant response [18], inhibition of proinflammatory agents [33], regulation of fibrotic formation, regulation of some growth factor expression [34], modulation of cell cycle genes, and reduction of adhesion molecules [35].

In one study, researchers sought to determine how oral administration of diclofenac sodium and ellagic acid affected the development of postoperative adhesions in rats. Ellagic acid, a powerful antioxidant and anti-inflammatory, inhibited adhesion in the experimental investigation by lowering oxidative stress on the establishment of peritoneal adhesion. Additionally, it was shown that ellagic acid has stronger anti-adhesion properties than diclofenac sodium [36]. In a study evaluating the effect of EA on the fibrotic phenotypes of hypertrophic scar fibroblasts (HSF), the main cells in hypertrophic scar formation, EA was shown to inhibit the proliferation and migration of HSFs and reduce collagen expression in a dose-dependent manner. Furthermore, EA was also found to reverse the upregulation of TGFβ1-induced Smad2/3 activation [37]. With these findings, it was proven that EA had an anti fibrotic effect on HSFs by blocking the TGFβ1/Smad2/3 pathway. In one study, EA was shown to effectively reduce bleomycin-induced pulmonary fibrosis by promoting autophagy and apoptosis of myofibroblasts in mice [38]. In a study examining the effects of EA on rats with a myocardial infarction model, it was shown that EA significantly reduced the area of cardiac fibrosis, mRNA expression of HDAC1, collagen-1, collagen-3, MMP-2 and − 9 in the myocardial infarction model. The same study found that EA at a dose of 60 mol/L reduced the expression of the proteins collagen I, collagen III, HDAC1, MMP-2, and − 9 and reduced cell proliferation and migration [38]. In one study, immortalized Human Cardiac Fibroblasts were stimulated with 10 ng/mL TGF-B1 for 24 h to induce a fibrotic injury. To investigate the fibrotic effects of EA, the levels of some proteins were examined. In the study, ellagic acid was shown to inhibit TGF-β1-Smad-2/3-MMP2/9 and Wnt/β-catenin

signaling through Nrf2 activation [39]. In a study investigating the therapeutic effect of EA on diabetic kidney damage, researchers showed that the fibrotic structure in DM groups was reduced by EA application with Masson trichrome staining. In addition, it was shown that the expression levels of TGFB1, psmad3, and aSMA, which are involved in the fibrotic pathway, were significantly reduced in the EA-treated group compared to the DM group [40]. In a study evaluating pancreatic fibrosis in rats, TGFβ1 mRNA expression was shown to be decreased in rats treated with EA (100 mg/kg/day) [41]. In our study, EA was applied at a dose of 100 mg/kg/day for 35 days as a therapeutic agent in the IUA model, which we created by applying mechanical damage to the uterus. With our Masson trichrome staining results, it was shown that fibrosis decreased in the groups treated with EA. In addition, as a result of protein and gene analyses, it was observed that the expression of TGFβ1 related to the formation of fibrotic structures, decreased with EA treatment. BMP7 activity was reduced, which mediates a mechanism opposite to TGF-mediated profibrogenic signaling.

Leukemia inhibitory factor (LIF), an interleukin (IL)− 6 family cytokine, is known to have a significant role in controlling uterine receptivity [42,43]. Epithelial-mesenchymal transition, angiogenesis, stromal cell decidualization, cell proliferation, and integrin signaling are only a few of the mechanisms that LIF activates to produce its effects [42]. In a study, it was shown that paeoniflorin, which is used as an agent, increases endometrial receptivity by inducing LIF [44]. In this study, we looked at how EA, a substance that can increase endometrial receptivity, affected LIF expression. In our investigation, IUA model rats showed considerably lower levels of LIF gene and protein expression compared to the control group. However, it was shown that EA therapy greatly enhanced the level of LIF in the tissue.

5. Conclusion

The results of this study conclude that EA used as a treatment for IUA promotes uterine tissue healing by reducing fibrosis and increases implantation rates by increasing endometrial receptivity. The results of this study will shed light on the molecular studies required to create a treatment against IUA and will enable the development of current treatment approaches.

Funding

This work was supported by the Scientific Researches Project Unit at Near East University [grant number GRN-2019–1–001].

CRediT authorship contribution statement

Saribas GS: Conceptualization, Methodology, Formal analysis, Investigation, Resources, Writing – original draft. **Akarca Dizakar O:** Conceptualization, Methodology, Investigation. **Ozogul C:** Investigation, Writing – review & editing, Investigation. **Celik E:** Methodology, Writing – original draft, Formal analysis. **Ergoren MC:** Formal analysis, Methodology, Writing – review & editing.

Declaration of Competing Interest

The authors declare that they have no known competing financial interests or personal relationships that could have appeared to influence the work reported in this paper.

Availability of supporting data

Data will be made available on request.

References

[1] J.G. Asherman, Amenorrhoea traumatica (atretica), BJOG 55 (1) (1948) 23–30, https://doi.org/10.1111/j.1471-0528.1948.tb07045.x.
[2] L. Kou, X. Jiang, S. Xiao, Y.-Z. Zhao, Q. Yao, R. Chen, Therapeutic options and drug delivery strategies for the prevention of intrauterine adhesions, J. Control. Release 318 (2020) 25–37, https://doi.org/10.1016/j.jconrel.2019.12.007.
[3] J. T.u, N.B. Kaitu'u-Lino, L.A. Morison, Salamonsen, Estrogen is not essential for full endometrial restoration after breakdown: lessons from a mouse model, Endocrinology 148 (10) (2007) 5105–5111, https://doi.org/10.1210/en.2007-0716.
[4] L.A. Salamonsen, Tissue injury and repair in the female human reproductive tract, Reproduction 125 (3) (2003) 301–311, https://doi.org/10.1530/rep.0.1250301.
[5] A. Conforti, C. Alviggi, A. Mollo, G. De Placido, A. Magos, The management of Asherman syndrome: a review of literature, Reprod. Biol. Endocrinol. 11 (1) (2013) 118, https://doi.org/10.1186/1477-7827-11-118.
[6] J.H. Yang, C.D. Chen, S.U. Chen, Y.S. Yang, M.J. Chen, The influence of the location and extent of intrauterine adhesions on recurrence after hysteroscopic adhesiolysis, BJOG 123 (4) (2016) 618–623, https://doi.org/10.1111/1471-0528.13353.
[7] E.A. Evans-Hoeker, S.L. Young, Endometrial receptivity and intrauterine adhesive disease, Semin. Reprod. Med. 32 (05) (2014) 392–401, https://doi.org/10.1055/s-0034-1376358.
[8] Z. Tao, H. Duan, Expression of adhesion-related cytokines in the uterine fluid after transcervical resection of adhesion, Zhonghua Fu Chan Ke Za Zhi 47 (10) (2012) 734–737.
[9] X. Santamaria, S. Cabanillas, I. Cervello, C. Arbona, F. Raga, J. Ferro, J. Palmero, J. Remohí, A. Pellicer, C. Simón, Autologous cell therapy with CD133+ bone marrow-derived stem cells for refractory Asherman's syndrome and endometrial atrophy: a pilot cohort study, Hum. Reprod. 31 (5) (2016) 1087–1096, https://doi.org/10.1093/humrep/dew042.
[10] L. Gao, Z. Huang, H. Lin, Y. Tian, P. Li, S. Lin, Bone marrow mesenchymal stem cells (BMSCs) restore functional endometrium in the rat model for severe Asherman syndrome, Reprod. Sci. 26 (3) (2019) 436–444, https://doi.org/10.1177/1933719118799201.
[11] Z.-M. Hao, M. Cai, Y.-F. Lv, Y.-H. Huang, H.-H. Li, Oral administration of recombinant adeno-associated virus-mediated bone morphogenetic protein-7 suppresses CCl4-induced hepatic fibrosis in mice, Mol. Ther. 20 (11) (2012) 2043–2051, https://doi.org/10.1038/mt.2012.148.
[12] B.-L. Chen, J. Peng, Q.-F. Li, M. Yang, Y. Wang, W. Chen, Exogenous bone morphogenetic protein-7 reduces hepatic fibrosis in Schistosoma japonicum-infected mice via transforming growth factor-β/Smad signaling, World J. Gastroenterol. 19 (9) (2013) 1405, https://doi.org/10.3748/wjg.v19.i9.1405.
[13] R. Weiskirchen, S.K. Meurer, BMP-7 counteracting TGF-beta1 activities in organ fibrosis, Front. Biosci. 18 (4) (2013) 1407–1434, https://doi.org/10.2741/4189.
[14] A. González-Sarrías, J.C. Espín, F.A. Tomás-Barberán, M.T. García-Conesa, Gene expression, cell cycle arrest and MAPK signalling regulation in Caco-2 cells exposed to ellagic acid and its metabolites, urolithins, Mol. Nutr. Food Res. 53 (6) (2009) 686–698, https://doi.org/10.1002/mnfr.200800150.
[15] M.-Y. Kuo, H.-C. Ou, W.-J. Lee, W.-W. Kuo, L.-L. Hwang, T.-Y. Song, C.-Y. Huang, T.-H. Chiu, K.-L. Tsai, C.-S. Tsai, Ellagic acid inhibits oxidized low-density lipoprotein (OxLDL)-induced metalloproteinase (MMP) expression by modulating the protein kinase C-α/extracellular signal-regulated kinase/peroxisome proliferator-activated receptor γ/nuclear factor-κB (PKC-α/ERK/PPAR-γ/NF-κB) signaling pathway in endothelial cells, J. Agric. Food Chem. 59 (9) (2011) 5100–5108, https://doi.org/10.1021/jf1041867.
[16] S. Polce, C. Burke, L. França, B. Kramer, A.M.D.A. Paes, M. Carrillo-Sepulveda, Ellagic acid alleviates hepatic oxidative stress and insulin resistance in diabetic female rats, Nutrients 10 (5) (2018) 531, https://doi.org/10.3390/nu10050531.
[17] G.S. Saribas, C. Ozogul, M. Tiryaki, F.A. Pinarli, S.H. Kilic, Effects of uterus derived mesenchymal stem cells and their exosomes on Asherman's syndrome, Acta Histochem 122 (1) (2020), 151465, https://doi.org/10.1016/j.acthis.2019.151465.
[18] S.Ö. Akarca Dizakar, G.S. Saribas, A. Tekcan, Effects of ellagic acid in the testes of streptozotocin induced diabetic rats, Drug Chem. Toxicol. 45 (5) (2021) 2123–2130, https://doi.org/10.1080/01480545.2021.1908714.
[19] M. Tasaki, T. Umemura, M. Maeda, Y. Ishii, T. Okamura, T. Inoue, Y. Kuroiwa, M. Hirose, A. Nishikawa, Safety assessment of ellagic acid, a food additive, in a subchronic toxicity study using F344 rats, Food Chem. Toxicol. 46 (3) (2008) 1119–1124, https://doi.org/10.1016/j.fct.2007.10.043.
[20] P. Malini, G. Kanchana, M. Rajadurai, Antibiabetic efficacy of ellagic acid in streptozotocin-induced diabetes mellitus in albino wistar rats, Asian J. Pharm, Clin. Res. 4 (3) (2011) 124–128.
[21] E. Dreisler, J.J. Kjer, Asherman's syndrome: current perspectives on diagnosis and management, Int. J. Women's. Health 11 (2019) 191, https://doi.org/10.2147/IJWH.S165474.
[22] C.M. March, Management of Asherman's syndrome, Reprod. Biomed. Online 23 (1) (2011) 63–76, https://doi.org/10.1016/j.rbmo.2010.11.018.
[23] E. Puente Gonzalo, L. Alonso Pacheco, A. Vega Jiménez, S.G. Vitale, A. Raffone, A. S. Laganà, Intrauterine infusion of platelet-rich plasma for severe Asherman syndrome: a cutting-edge approach, Updates Surg. 73 (6) (2021) 2355–2362, https://doi.org/10.1007/s13304-020-00828-0.
[24] C. Gargett, Uterine stem cells: what is the evidence? Hum. Reprod. Update 13 (1) (2006) 87–101, https://doi.org/10.1093/humupd/dml045.

[25] J.G. Schenker, Etiology of and therapeutic approach to synechia uteri, Eur. J. Obstet. Gynecol. Reprod. Biol. 65 (1) (1996) 109–113, https://doi.org/10.1016/0028-2243(95)02315-j.
[26] P. Gambadauro, J. Gudmundsson, R. Torrejón, Intrauterine adhesions following conservative treatment of uterine fibroids, Obstet. Gynecol. Int (2012)) (2012), https://doi.org/10.1155/2012/853269.
[27] C.M. March, Intrauterine adhesions, Obstet. Gynecol. Clin. North Am. 22 (3) (1995) 491–505.
[28] H. Al-Inany, Intrauterine adhesions, Acta Obstet. Gynecol. Scand. 80 (11) (2001) 986–993.
[29] F. Hou, R. Liu, X. Liu, L. Cui, Y. Wen, S. Yan, C. Yin, Attenuation of liver fibrosis by herbal compound 861 via upregulation of BMP-7/Smad signaling in the bile duct ligation model rat, Mol. Med. Rep. 13 (5) (2016) 4335–4342, https://doi.org/10.3892/mmr.2016.5071.
[30] X.-M. Meng, A.C. Chung, H.Y. Lan, Role of the TGF-β/BMP-7/Smad pathways in renal diseases, Clin. Sci. 124 (4) (2013) 243–254, https://doi.org/10.1042/CS20120252.
[31] D. Merino, A.V. Villar, R. García, M. Tramullas, L. Ruiz, C. Ribas, S. Cabezudo, J. F. Nistal, M.A. Hurlé, BMP-7 attenuates left ventricular remodelling under pressure overload and facilitates reverse remodelling and functional recovery, Cardiovasc. Res. 110 (3) (2016) 331–345, https://doi.org/10.1093/cvr/cvw076.
[32] G. Yang, Z. Zhu, Y. Wang, A. Gao, P. Niu, L. Tian, Bone morphogenetic protein-7 inhibits silica-induced pulmonary fibrosis in rats, Toxicol. Lett. 220 (2) (2013) 103–108, https://doi.org/10.1016/j.toxlet.2013.04.017.
[33] D. Cornélio Favarin, M. Martins Teixeira, E. Lemos de Andrade, C. de Freitas Alves, J.E. Lazo Chica, C. Artério Sorgi, L.H. Faccioli, A. Paula, Rogerio, Anti-inflammatory effects of ellagic acid on acute lung injury induced by acid in mice, Mediat. Inflamm. (2013)) (2013), https://doi.org/10.1155/2013/164202.
[34] R. Kesavan, R. Ganugula, T. Avaneesh, U. Kumar, G.B. Reddy, M. Dixit, Ellagic acid inhibits PDGF-BB-induced vascular smooth muscle cell proliferation and prevents atheroma formation in streptozotocin-induced diabetic rats, J. Nutr. Biochem 24 (11) (2013) 1830–1839, https://doi.org/10.1016/j.jnutbio.2013.04.004.
[35] L. Labrecque, S. Lamy, A. Chapus, S. Mihoubi, Y. Durocher, B. Cass, M. W. Bojanowski, D. Gingras, R. Béliveau, Combined inhibition of PDGF and VEGF receptors by ellagic acid, a dietary-derived phenolic compound, Carcinogenesis 26 (4) (2005) 821–826, https://doi.org/10.1093/carcin/bgi024.
[36] T.D. Allahverdi, E. Allahverdi, S. Yayla, T. Deprem, O. Merhan, S. Vural, The comparison of the effects of ellagic acid and diclofenac sodium on intra-abdominal adhesion: an in vivo study in the rat model, Int. Surg. 99 (5) (2014) 543–550, https://doi.org/10.9738/INTSURG-D-14-00065.1.
[37] X. Liu, X. Gao, H. Li, Z. Li, X. Wang, L. Zhang, B. Wang, X. Chen, X. Meng, J. Yu, Ellagic acid exerts anti-fibrotic effects on hypertrophic scar fibroblasts via inhibition of TGF-β1/Smad2/3 pathway, Appl. Biol. Chem. 64 (1) (2021) 1–10, https://doi.org/10.1186/s13765-021-00641-2.
[38] X. Li, K. Huang, X. Liu, H. Ruan, L. Ma, J. Liang, Y. Cui, Y. Wang, S. Wu, H. Li, Ellagic Acid Attenuates BLM-Induced Pulmonary Fibrosis via Inhibiting Wnt Signaling Pathway, Front. Pharmacol. 12 (2021), 639574, https://doi.org/10.3389/fphar.2021.639574.
[39] F. Mannino, C. Imbesi, A. Bitto, L. Minutoli, F. Squadrito, T. D'Angelo, C. Booz, G. Pallio, N. Irrera, Anti-oxidant and anti-inflammatory effects of ellagic and punicic acid in an in vitro model of cardiac fibrosis, Biomed. Pharmacother. 162 (2023), 114666, https://doi.org/10.1016/j.biopha.2023.114666.
[40] G.S. Saribas, H.T. Yildiz, O. Gorgulu, Ellagic acid inhibits TGFβ1/smad-induced renal fibrosis in diabetic kidney, Inj., Duzce Med. J. 24 (3) (2022) 321–327, https://doi.org/10.18678/dtfd.1198021.
[41] N. Suzuki, A. Masamune, K. Kikuta, T. Watanabe, K. Satoh, T. Shimosegawa, Ellagic acid inhibits pancreatic fibrosis in male Wistar Bonn/Kobori rats, Dig. Dis. Sci. 54 (4) (2009) 802–810, https://doi.org/10.1007/s10620-008-0423-7.
[42] G.X. Rosario, C.L. Stewart, The multifaceted actions of leukaemia inhibitory factor in mediating uterine receptivity and embryo implantation, Am. J. Reprod. Immunol. 75 (3) (2016) 246–255, https://doi.org/10.1111/aji.12474.
[43] W. Hu, Z. Feng, A.K. Teresky, A.J. Levine, p53 regulates maternal reproduction through LIF, Nature 450 (7170) (2007) 721–724, https://doi.org/10.1038/nature05993.
[44] H.-R. Park, H.-J. Choi, B.-S. Kim, T.-W. Chung, K.-J. Kim, J.-K. Joo, D. Ryu, S.-J. Bae, K.-T. Ha, Paeoniflorin enhances endometrial receptivity through leukemia inhibitory factor, Biomolecules 11 (3) (2021) 439, https://doi.org/10.3390/biom11030439.